Indonesian Journal of Science & Technology

Journal homepage: http://ejournal.upi.edu/index.php/ijost/

Relationship between Shear Velocities Recorded by Microtremor Observations and Seismic Cone Penetration Test Results

Rusnardi Rahmat Putra[1*], *J. Kiyono*[2], *Sai K. Vanapalli*[3], *Y. Ono*[4]

[1]Faculty of Engineering, Universitas Negeri Padang, Jl Prof. Dr. Hamka, Padang, 25171, Indonesia
[2]Graduate School of Engineering, Urban Management Department, Katsura Campus, Kyoto University Nishikyo, Kyoto 615-8540, Japan
[3]Faculty of Engineering, Department of Civil Engineering, University of Ottawa, 161 Louis-Pasteur St. Room A015 (CBY) Ottawa ON K1N 6N5 Canada
4 Faculty of Engineering, Civil Engineering Department, Tottori University 4-101 Koyama Minami, Tottori city 680-8552, Japan

Correspondence: E-mail: rusnardi.rahmat@ft.unp.ac.id

ABSTRACT

This research proposes a relationship between two methods such as a numerical approach by conducting a microtremor array observation and field survey by using the seismic cone penetration test unit (SCPTu). A database of shear-wave velocity (Vs) measurements was established using the microtremor array technique and seismic cone penetration test unit (SCPTu) on high-quality samples of rock and soft soil in Padang city, Indonesia. The study also demonstrates that the Vs values obtained from the different methods are consistent with the microtremor array technique. This technique may thus be deemed a valuable tool, as it can be used in engineering practice with confidence. Comparison of the Vs for different soils at the first layer between the microtremor array observation results and the SCPTu results exhibited the microtremor array method is unable to determine the Vs at the layer where its Vs changes dramatically, such as at the same layer as station UNP at 2 to 3.5m deep.

ARTICLE INFO

Article History:
Submitted/Received 20 June 2020
First revised 19 March 2021
Accepted 14 May 2021
First available online 16 May 2021
Publication date 01 Sep 2021

Keywords:
Microtremor Array,
Shear Velocity,
Soil Characteristics.

1. INTRODUCTION

The location of Padang city is on the west coast of the island of Sumatra. The city is on the western part of Indonesia. It is situated nearby the Sumatran subduction zone and on the fault line formed on the Indo-Australian plate beneath the Eurasian plate. The plates' movement is about 50 to 70 mm/year. The plates activity is associated with the seismicity in the area (Genrich *et al*., 2000) and (Prawirodirdjo *et al*., 2000). The most recent earthquake in the Padang region occurred on 30 September 2009. The epicenter of this earthquake was in the ocean slab of the Eurasian plate of Indonesia at a depth of 80 km, specifically at -0.81°S, 99.65°E. It produced a ground motion that contributed to a high degree of shaking and tremors that were felt within a radius of approximately 923 km from the epicenter, including the Indonesian capital Jakarta as well as the neighboring countries of Malaysia and Singapore (Parker *et al*., 2020).

According to seismicity records, the fault line in the Sumatra island region contributes to destructive earthquakes. The earthquakes typically occur at shallow depths of 10 km to 100 km (**Figure 1**). This powerful earthquakes significantly affect the infrastructure, economy, and society of Padang (Putra *et al*., 2014). The average seismic shear-wave velocity from the surface to a depth of 30 meters (Vs30) is used as the fundamental parameter to build an earthquake-resistant building (Thein *et al*., 2015; Putra *et al*., 2017; Sutrisno *et al*., 2017). Seismic hazard and risk analyses for Padang city were conducted in 2012 (Putra *et al*., 2012; Putra *et al*., 2014), yielding data regarding local soil properties, especially the shear-wave velocity (Vs). The research was conducted at four surface accelerometer stations of the monitoring network.

The subsurface soil in the Padang has unconsolidated sediments as well as heterogeneous composition and properties (Lanin *et al*., 2019; Rosyidi *et al*., 2011). Numerous different methods were applied to obtain in situ Vs values to a target depth of at least 30 m, or the maximum capacity penetration of the cone: as much as 22 MPa for SCPTu. The techniques include seismic cone penetration tests (SCPT) with varying source offsets and microtremor array observation on Rayleigh waves with different processing approaches. SCPT proved to be a powerful and cost-effective approach in determining representative Vs profiles at the selected soil type (McGann et al., 2015; Pradono et al., 2019), such as soft soil for two stations (UNP and FTB) and a rock type for another (ADS).

The measured Vs profiles corresponded closely with the modeled profiles and significantly enhanced the ground motion model's derivation (Sofyan, 2016); moreover, the level of similarity between the theoretical transfer function from the Vs profile and the observed amplification from vertical array stations was excellent (Noorlandt *et al*., 2018), opposite from advantage, the used SPTu for this research is heavy to carry. This paper describes how this observation was conducted and how the procedures to attain clear information regarding the shear velocity (Vs), the relationship between the microtremor array results, and the seismic cone penetration unit (SCPTu).

DOI: https://doi.org/10.17509/ijost.v6i2.34191
p- ISSN 2528-1410 e- ISSN 2527-8045

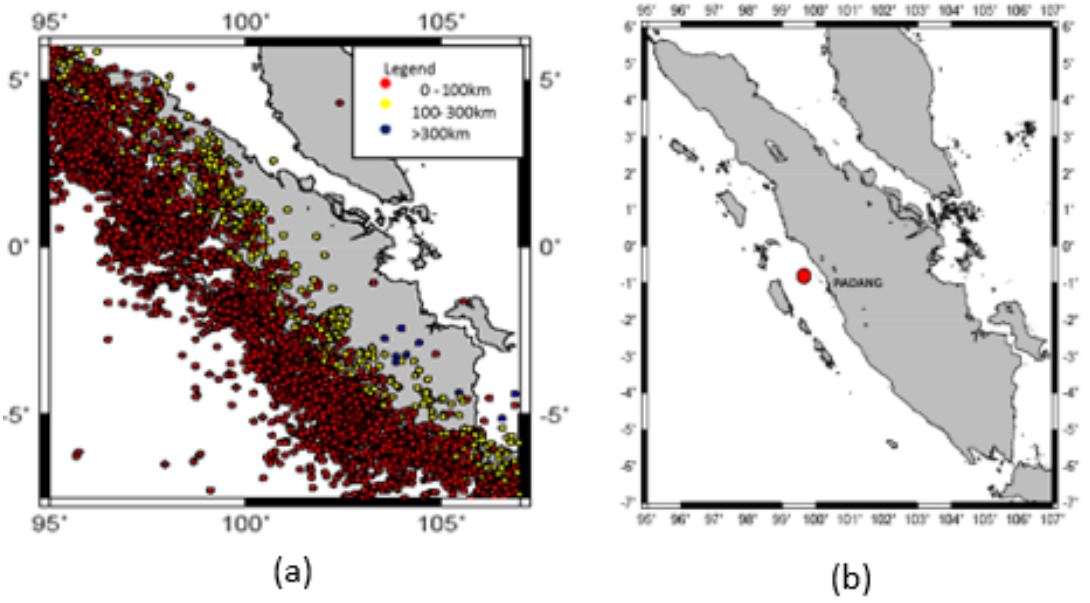

Figure 1. Seismicity details (a) Earthquake seismicity of Sumatra, Mw > 4 from 1779–2020 (b) the September 2009 Padang earthquake (red circle is the epicenter).

2. METHODS AND SETUP

2.1 Overview

The research was conducted in Padang City from 2009-2018. Padang is the capital city of West Sumatra province, Indonesia. The location of Padang city is at 100.38°E, 0.95°S. The main part of Padang city is located on an alluvial plain between the Indian Ocean (offshore) and the mountains. Almost all the mountainous area is composed of tertiary sedimentary rocks, with outcrops of metamorphic rocks in some places (ONO *et al*., 2012) and (Putra, 2020b). The alluvial plain spreads along the base of the mountains and is roughly 10 km wide in the east-west direction and 20 km wide in the north-south direction (**Figure 2**). The shallow subsurface in the Padang city region is of heterogeneous composition as a result of the microtremor array observation from a previous study.

The location of this city is between the the Indian Ocean, the Sunda Trench fault, and the Sumatran fault. The two faults are active. The slip rates of the faults are from 10 to 27 mm/year (natawidjaja & triyoso, 2007) and (Sieh & Natawidjaja, 2000). Based on our records, there are 2,995 events occurred in this region with a magnitude greater than four from AD 1779 to 2010 (Putra, R.R *et al*., 2014; Putra, R.R 2020). There were seven giant earthquakes occured in this area. One of the earthquake was in 2009 Padang. The earthquake was located in the ocean slab of the Indo-Australian plate. It caused extensive shaking and damage to houses and buildings in Padang and Padang Pariaman, due to the epicenter location (Juliafad *et al*., 2021). Its epicentre was about 60 km offshore from Padang (**Figure 1.b**). Fortunately, the earthquake did not generate a tsunami given that it was an intra-slab earthquake. It was also at intermediate depth with comparable magnitude.

DOI: https://doi.org/10.17509/ijost.v6i2.34191
p- ISSN 2528-1410 e- ISSN 2527-8045

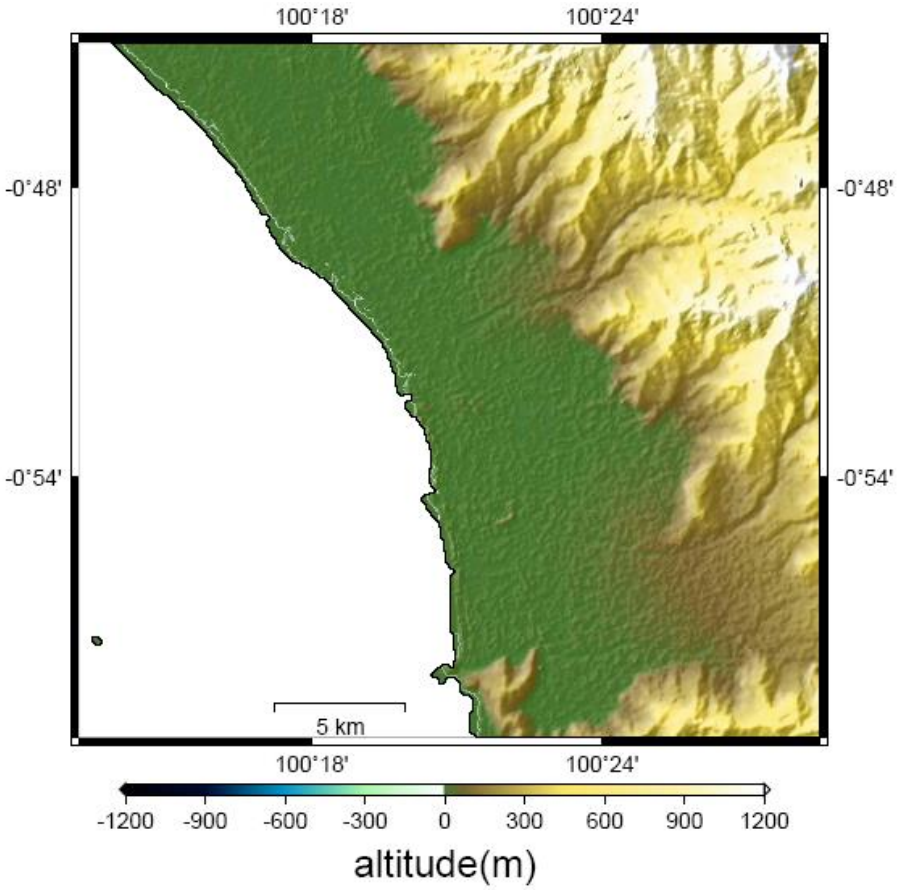

Figure 2. Topography of Padang.

A database of shear-wave velocity (Vs) measurements using the microtremor array technique and the seismic cone penetration test unit (SCPTu) on high-quality samples for rock and soft soil in Padang region sites has been established. Experimental microtremor studies were also verified using the analytical model proposed by (Tavakoli *et al.*, 2016), which provided reasonably good comparison of Vs for the subterraneous alluvium. The SCPTu results proved to be a useful and cost-effective approach in determining representative values of Vs. The purpose of this study was to evaluate the different methods of measuring Vs, as well as to develop guidelines and correlations to assist in estimating the Vs profiles of clayey soils in Padang and nearby regions in the absence of site-specific data. Such relationships can be used in first-order estimates of Vs values from conventional soil properties. It was found that reliable and reproducible measurements of Vs can be obtained from the microtremor array technique for use in practical engineering applications.

The Vs values obtained from the different methods are similar to the data derived from the microtremor array technique (Putra *et al.*, 2014), such as from field survey studies suggesting that the SCPTu method is a convenient, fast and fairly accurate method to derive Vs values (Khazaei, Amiri & Khalilpour, 2017) and (Thornley *et al.*, 2019). A summary of the survey setup for the two different shear-wave methods is presented in **Table 1**.

DOI: https://doi.org/10.17509/ijost.v6i2.34191
p- ISSN 2528-1410 e- ISSN 2527-8045

Table 1. Summary of survey setup for the two different shear-wave methods.

	SCPT	Microtremor array
Sources	Steel beam and sledgehammer at 2.5m	Ambient noise
Receiver	Three component accelerometers in SCPT cone	Three component acceleration sensors, GPL-6A3P,
Remark	Vertical sample interval, max 1.0 m, coinciding with stratigraphical translation	Recording of ambient noise at 1, 3, 7 and 30 m for one station. Sampling frequency is 100 Hz and 200 Hz; recording ground motion duration from 10 to 30 minutes.
Depth of investigation	4-18m	Up to -102m and ~
Lateral average	2.5 m	Up to 30m
Vertical resolution	High, except shallow part	Medium decreasing with depth

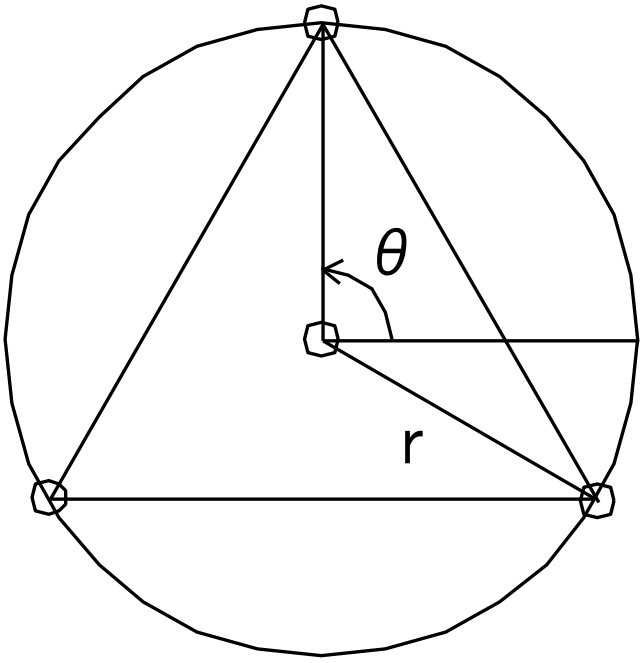

Figure 3. A four-point array observation.

2.2 Microtremor Array Observations

We conducted microtremor array investigations on 12 sites in several districts in Padang (**Figure 4**). The sampling frequency used was 100 Hz and 200 Hz, with recording ground motion duration from 10 to 30 minutes and an array radius from 1m up to 1km for each observation. **Figure 3** provides a succinct summary of the four-point array technique used in the present study. The site coordinates are 0°54'46.7"S, 100°27'53.7E", 0°55'45.3"S 100°21'26.5"E, and 0°53'52.1"S, 100°20'56.2"E for ADS, FTB and UNP respectively.

We followed the SPAC method to calculate the dispersion curves to estimate a velocity structure from the microtremor recordings (Nakamura, 2000; Carniel, Barazza & Pascolo, 2006). In this study, we

DOI: https://doi.org/10.17509/ijost.v6i2.34191
p- ISSN 2528-1410 e- ISSN 2527-8045

used the SPAC methods only. SPAC is a method of calculating the phase velocity from different frequencies of the Bessel function by taking the average of the normalized coherence function. It is defined as the spectrum from a site pair on the array.

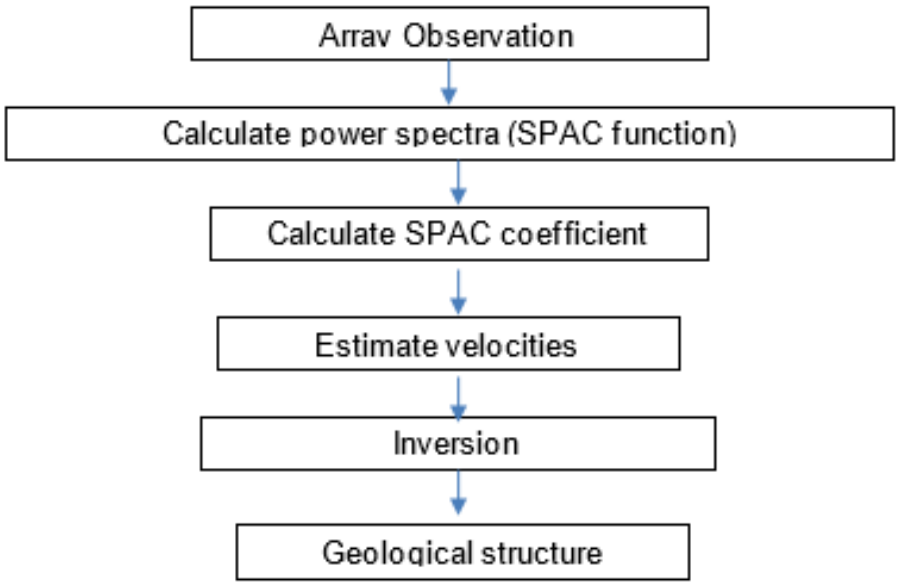

Figure 4. SPAC method flow chart.

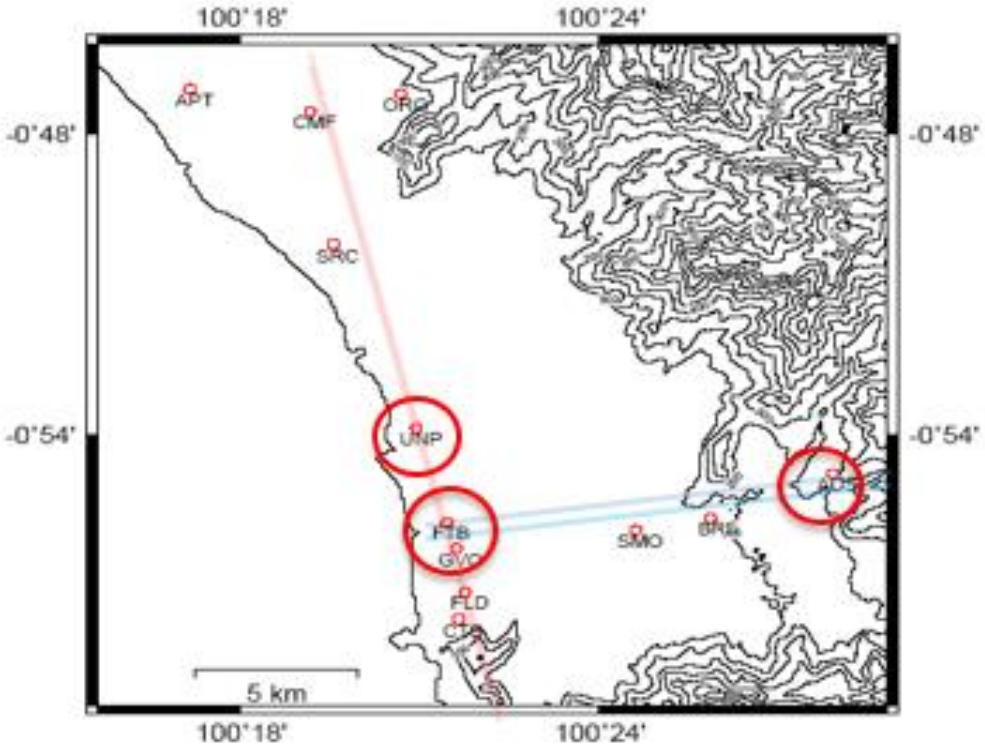

Figure 5. The 12 array observation sites; red circles are the compared observation stations ADS (right), FTB and UNP (left).

DOI: https://doi.org/10.17509/ijost.v6i2.34191
p- ISSN 2528-1410 e- ISSN 2527-8045

The outline of the SPAC method for the phase velocity calculation of Rayleigh waves is as follows:

$$F(\omega) = \frac{1}{2\pi}\int_{-\infty}^{\infty} f(t)\cdot exp(-i\omega t) = A_f(\omega)\cdot exp\left(-i\emptyset_f(\omega)\right) \quad (1)$$

$$G(\omega) = \frac{1}{2\pi}\int_{-\infty}^{\infty} g(t)\cdot exp(-i\omega t)\,dt = A_g(\omega)exp\left(-i\emptyset_g(\omega)\right) \quad (2)$$

$A_f(\omega)$, $A_g(\omega)$ and $\emptyset_f$ are differences between the amplitude of $\emptyset_g(\omega)$, $F(\omega)\ and\ G(\omega)$,respectively. Futher cross-correlation in the frequency region of the two waveforms will be as follows:

$$CC_{fg} = F(\omega)\cdot \overline{G(\omega)} = A_f(\omega)\cdot A_g(\omega)\cdot exp\left(i\Delta\emptyset(\omega)\right) \quad (3)$$

This shows the phase difference of$\Delta\emptyset(\omega)$

$$\Delta\emptyset(\omega) = \frac{\omega r}{c(\omega)} \quad (4)$$

$c(\omega)$ is the phase velocity from the phase difference.

$$CC_{fg} = A_f(\omega)\cdot A_g(\omega)\cdot exp\left(i\frac{\omega r}{c(\omega)}\right) \quad (5)$$

The complex coherence of two waveforms is defined by the following equation:

$$COH_{fg}(\omega) = \frac{CC_{fg}(\omega)}{A_f(\omega)\cdot A_g(\omega)} = ex\,p\left(i\frac{\omega r}{c(\omega)}\right) \quad (6)$$

$$Re\left(COH_{fg}(\omega)\right) = \cos\left(i\frac{\omega r}{c(\omega)}\right) \quad (7)$$

$$c(\omega,\varphi) = \frac{c(\omega)}{cos\varphi} \quad (8)$$

$$SPAC(\omega,r) = \frac{1}{2\pi}\int_0^{2\pi} exp(i\frac{\omega r}{c(\omega)}cos\varphi)d\varphi \quad (9)$$

(10)

$$Re\big(SPAC(\omega,r)\big) = \frac{1}{2\pi}\int_0^{2\pi} \cos(i\frac{\omega r}{c(\omega)}cos\varphi)d\varphi\ J\left(\frac{\omega r}{c(\omega)}\right) = \frac{1}{2\pi}\int_0^{2\pi} exp(\frac{\omega r}{c(\omega)}cos\varphi)d\varphi \quad (11)$$

where Jo(x) is the zero-order Bessel function of the first x, and c(ω) is the phase velocity at ω frequency. The SPAC coefficient ρ(r,ω) can be taken from the frequency domain using the Fourier series transformation of the observed microtremors. From the SPAC coefficient ρ(r,ω), the phase velocity is calculated for different frequencies from the Bessel function. Equation 11 and the velocity model can be inverted. The layer thickness and the average S-wave velocity at each array site can be estimated. The average S wave velocity model was obtained by taking the average of the estimated ground structure of the array site. It was calculated by a weighted average using an S-wave velocity structure for a weighted layer thickness.

$$Re\big(SPAC(\omega,r)\big) = J\left(\frac{\omega r}{c(\omega)}\right) \quad (12)$$

From the SPAC coefficient ρ(r,ω), the phase velocity is calculated for every frequency from the Bessel function argument of equation 12, and the velocity model can be inverted. The layer thickness and the average S-wave velocity for each array site were determined. The average S-wave velocity model, obtained by averaging the estimated ground structure of the array site. It was calculated by a weighted average using an S-wave velocity structure estimated as a weighted layer thickness. **Figure 7** shows an example of the dispersion curve obtained using the array observations.

DOI: https://doi.org/10.17509/ijost.v6i2.34191
p- ISSN 2528-1410 e- ISSN 2527-8045

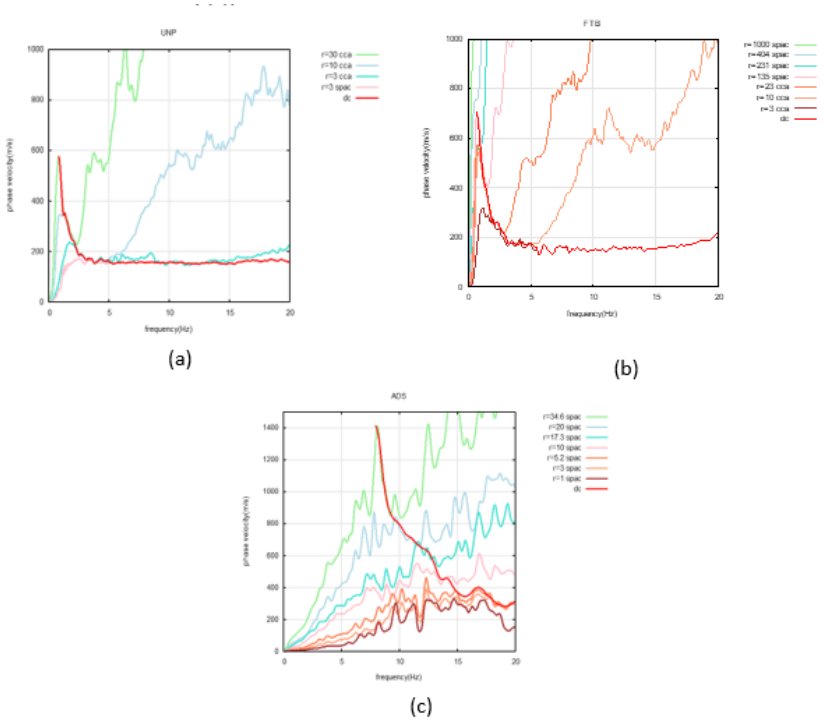

Figure 6. Phase velocity from SPAC and CCA method at several sites in Padang, (a) Station FTB, (b) Station UNP and (c) ADS.

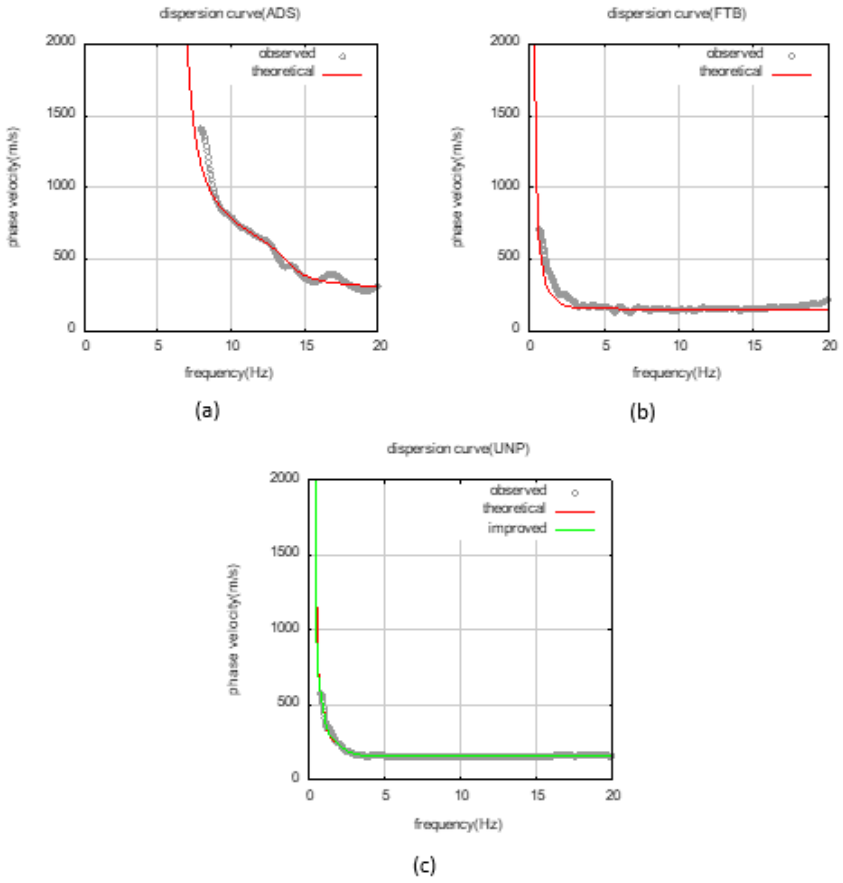

Figure 7. Dispersion curve at several sites in Padang; (a) Rock at station ADS, (b) Soft type at station FTB, (c) Soft type at station UNP.

DOI: https://doi.org/10.17509/ijost.v6i2.34191
p- ISSN 2528-1410 e- ISSN 2527-8045

By conducting an inversion analysis using the particle swarm optimization (PSO) algorithm on the above dispersion curves, the subsurface structure beneath the site can be estimated. The PSO is a solution method for a non-linear optimization problem (Chopard & Tomassini, 2018). We estimated the subsurface structure of the model by minimizing the difference between the observed and theoretical phase velocity curves. We estimated the subsurface structure of the model by solving a nonlinear minimization problem with the fitness function below.

$$v_{id}^{t+1} = \omega\, v_{id}^{t} + c_1 r_1 (p_{id}^{t} - x_{id}^{t}) + c_2 r_2 (p_{gd}^{t} - x_{gd}^{t}) \quad (13)$$

$$x_{id}^{t+1} = x_{id}^{t} + v_{id}^{t+1} \quad (14)$$

where v_{id}^{t} is the particle velocity of the i^{th} component in dimension d in the interaction, x_{id}^{t} is the particle position of the i^{th} component in dimension d in the interaction, c_1 and c_2 are constant weight factors, p_i is the best position achieved by particle i, p^g is the best position found by the neighbour of particle i, $r_1$and r_2 are random factors in the [0,1] interval and ω is the inertia weight. Before performing the inversion analysis, the subsurface structure was assumed to consist of horizontal layers of elastic and homogeneous media above a semi-infinite elastic body. The shear wave velocity and thickness of each layer are the parameters determined by the inversion analysis. The results enabled us to determine the condition of shallow subsurface structures (Kiyono *et al*., 2011). The outline of the SPAC method for the phase velocity calculation of the Rayleigh waves is shown in **Figure 3 and 4**.

2.3 Determination of Layer Thickness

The peaks in the short and long periods of the observed H/V spectrum could be explained by the estimated subsurface soil structure. In this study, we used the two distinct peaks in the observed H/V spectra and V_s structure obtained by array observation. The technique used was the 1/4 wavelength principle, which can approximately be extended to multi-layered media.

$$H^* = \frac{T_p}{4} \frac{\sum_{i=1}^{n} V_{S_i} \cdot H_i}{\sum_{i=1}^{n} H_i} \quad (15)$$

where H is a thickness of a layer. Here we divided the ground into three layers: the upper two layers and a base semi-infinite layer. The range of the shear wave velocity for the first, second and third layers was assumed: (I) Vs $\leqq$ 300 m/s; (II) 300 < Vs < 300 m/s; (III) Vs $\geqq$ 3000 m/s.

The target area is shown in **Figure 8(a)**, in which the rapidly varying area of the subsurface condition and dense observation area are enclosed. The ground model was constructed as follows: the rectangular area (about 10 km x10 km) in **Figure 8(a)** was divided into100*100 meshes (100 m square). According to the Kriging technique, the values of predominant periods Ts and T at the centre of each mesh are interpolated by using the finite number of peak periods read from the observed H/V spectrum.

In **Figure 9 (a)** at station ADS shows the Vs from 0-4m depth is average 308.8m/s corresponds to relatively rock type and (b) at station FTB from the Vs from 0- 18 m (green line) is average 169.3m/s and at station UNP from the Vs from 0- 16 m (yellow line) is average 169m/s correspond to relatively soft type at the first layer.

Three of the 12 observation sites were considered for evaluating the relationship, one each for rock at station ADS (Vs > 300m/s) and two for soft soil at FTB and UNP (Vs < 200m/s) (**Figure. 5**).

3. Seismic Cone Penetration Test unit (SCPTu)

DOI: https://doi.org/10.17509/ijost.v6i2.34191
p- ISSN 2528-1410 e- ISSN 2527-8045

Seismic cone penetration tests (SCPTu) consist of a normal CPT with an accelerometer contained in the cone. The cone penetrates into the soils until it reaches defined depth intervals for a Vs measurement. Shear waves were generated at the surface by striking a 10 kg sledgehammer on opposite sides of 2.5 m hardwood beams. The cone penetration is typically stopped every 1.0 m and the source is located ~ 1 m from the entry point at the surface (Noguchi *et al.*, 2010) (**Figure 7**). The seismic cone penetration test unit (SCPTu) used for seismic data acquisition was the BCE SC1-DACtm 2013. The field conducted survey method as shown in **Figure 10**.

Three stations were compared based on the soil type result from the microtremor testing: soft type (Vs<200m/s) for the FTB, UNP station and rock type (Vs>200) for the ADS station. The considered depth of the surface structure for each site was 4 m for ADS, 18 m for FTB and 16 m for UNP because the cone could not penetrate further having reached the maximum capacity of as much as 22 MPa. At every 1 m increment, a ground motion wave form was obtained and the recorded data were converted to the frequency domain using the fast Fourier transform (FFT) method (**Figure 11**).

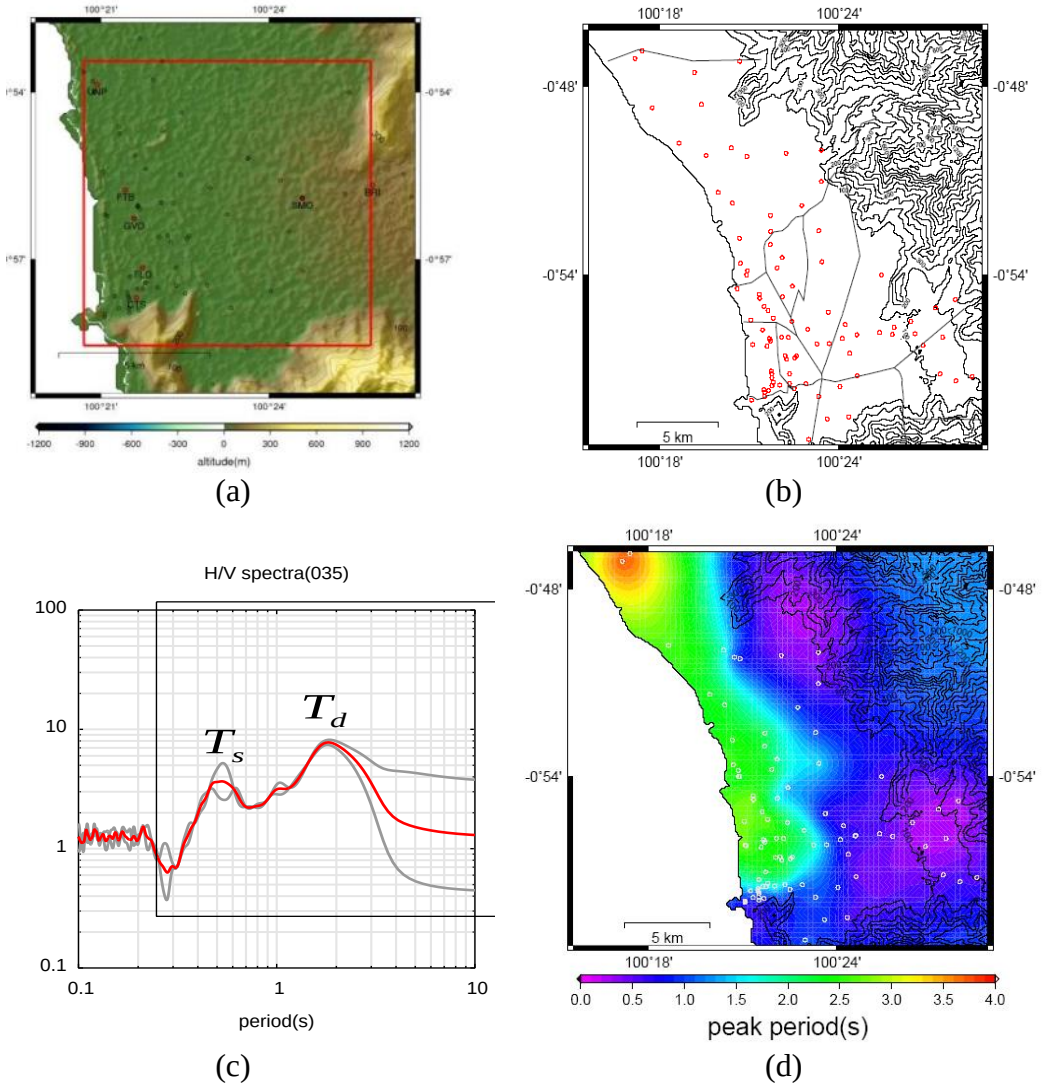

DOI: https://doi.org/10.17509/ijost.v6i2.34191
p- ISSN 2528-1410 e- ISSN 2527-8045

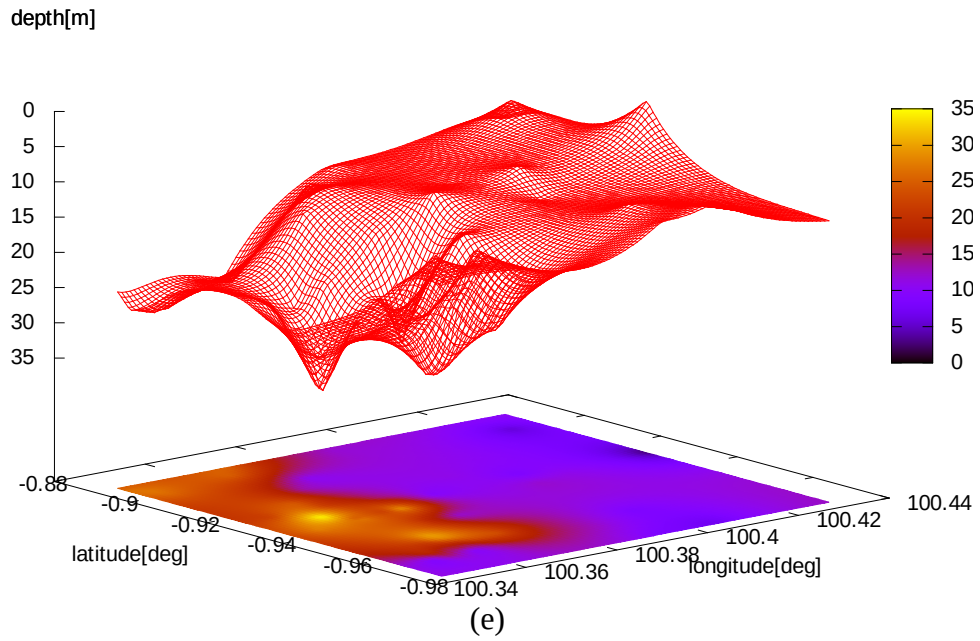

(e)

Figure 8. Three dimensional shape of the estimated subsurface structure: (a) target area for the analysis of three layered model, (b) Observation sites for microtremor single observation, (c) sample of H/V spectrum, and (d) H/V distribution for whole Padang city and (e) boundary depth for one layer.

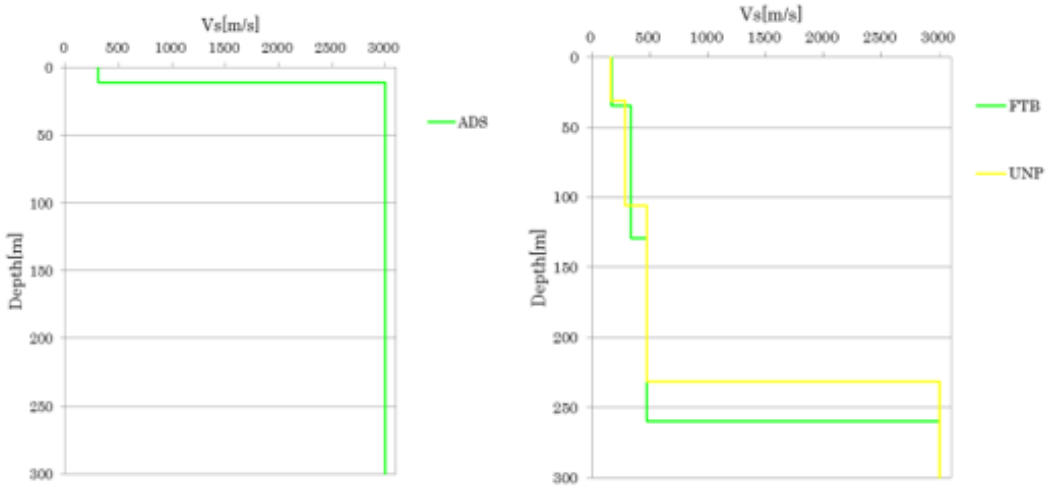

Figure 9. Microtremor array results for three stations in Padang: (a) results for station ADS (rock type) and (b) FTB and UNP stations (soft type).

DOI: https://doi.org/10.17509/ijost.v6i2.34191
p- ISSN 2528-1410 e- ISSN 2527-8045

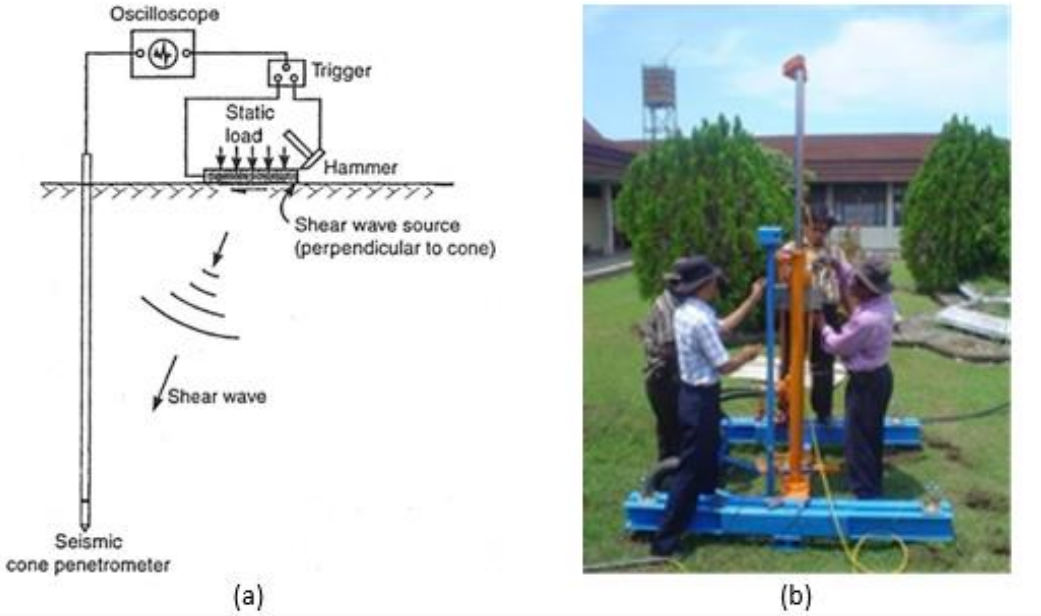

Figure 10. Illustration: (a) SCPTu observation mechanism, (b) setting up the SCTPu device.

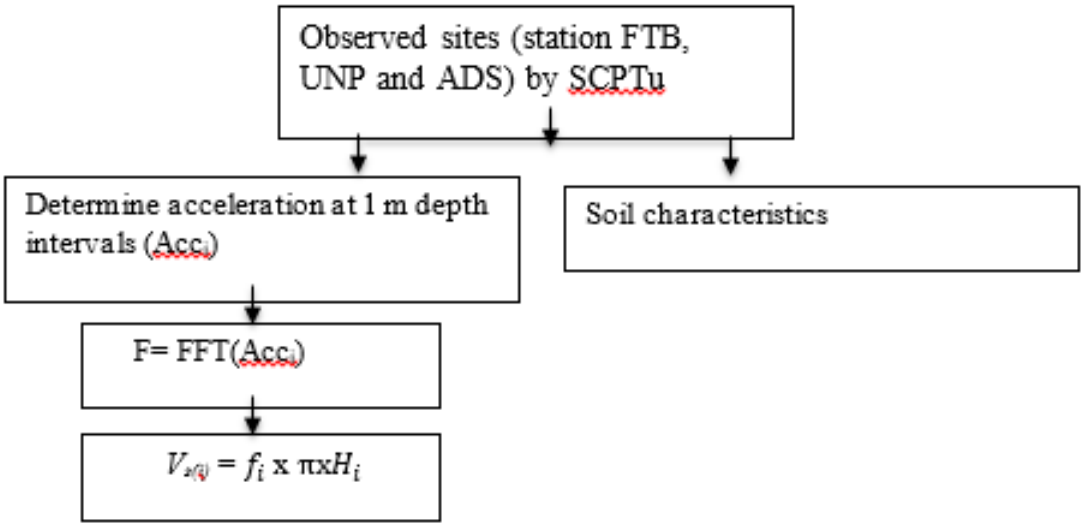

Figure 11. Flow chart to highlight the procedure followed in order to estimate V_s from SCPTu.

Table 2 shows the comparison of Vs results. The Vs was determined from the SCPTu for every 1 m increment depth using Equation (16) (Wang *et al.*, 2018) by following a single layer model according to a simplified single degree of freedom system. The considered layer is the first layer only, where Hi = 1 m increment, ρ_i=1.7 ton/m3 and T_i is estimated from the FFT of recorded ground motion at every 1 metre increment result as shown in **Figure 13-17**.

$$T = \pi \sum_{=1}^{n} \frac{h_i}{V_i} \qquad (16)$$

where *T* is the frequency obtained from FFT from the recorded acceleration for each depth 1 m, and H is the depth from the

DOI: https://doi.org/10.17509/ijost.v6i2.34191
p- ISSN 2528-1410 e- ISSN 2527-8045

surface. Figures 13-17 summaries the results of various soil properties from the data generated from SCPTu.

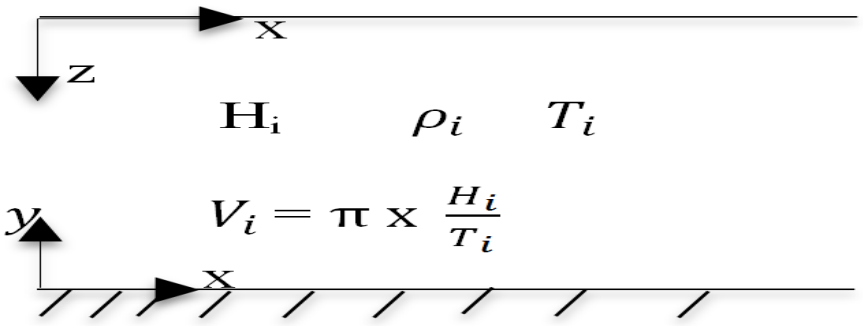

Figure 12. Single shear velocity model.

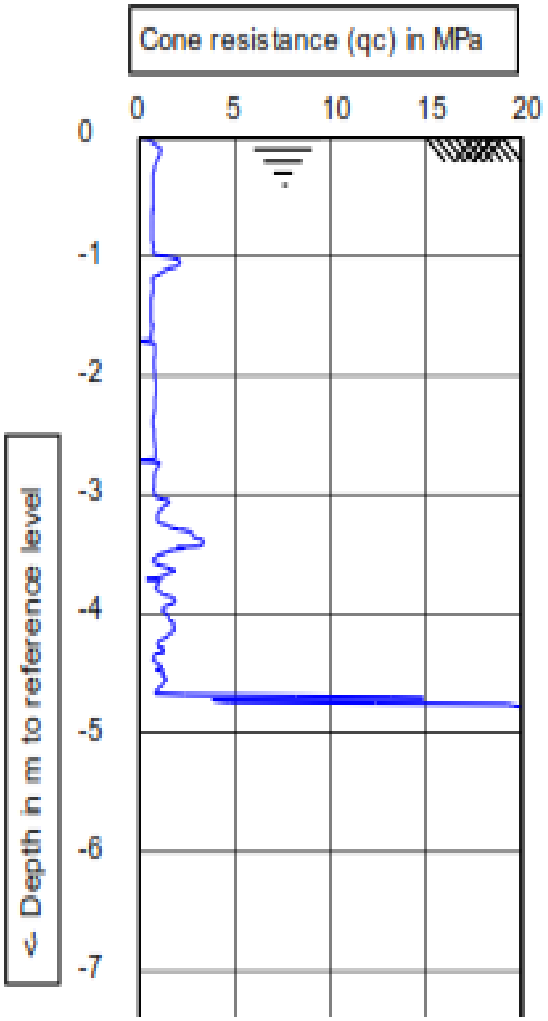

Figure 13. CPT data for station ADS: (a) CPT sounding of SCPT at ADS with cone resistance.

DOI: https://doi.org/10.17509/ijost.v6i2.34191
p- ISSN 2528-1410 e- ISSN 2527-8045

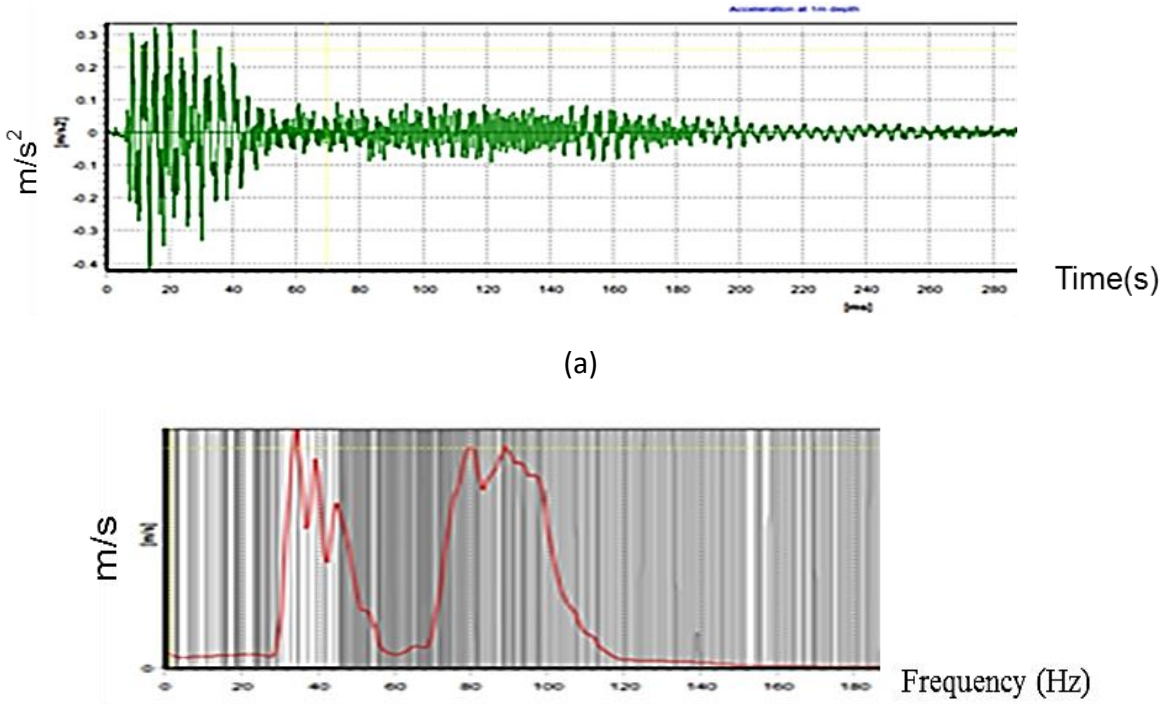

Figure 14. SCPT data for station ADS: (a) acceleration at 1 m depth and (b) frequency at 1 m depth (from FFT).

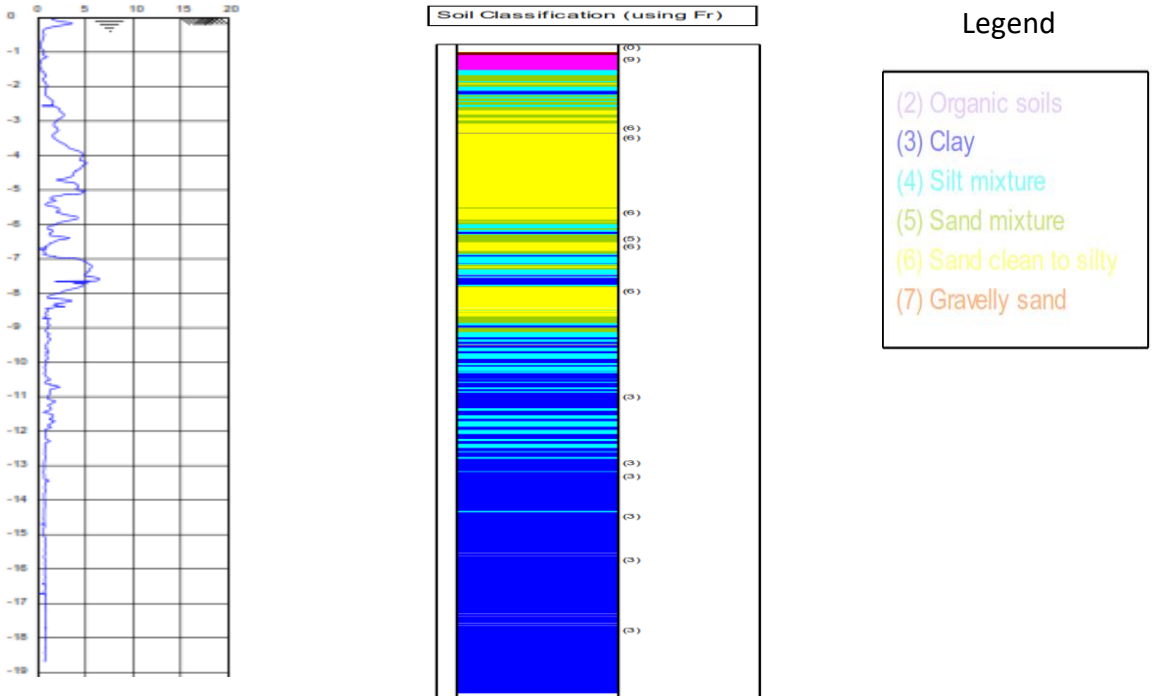

Figure 15. CPT data for station FTB: (a) CPT sounding of SCPTu with cone resistance.

DOI: https://doi.org/10.17509/ijost.v6i2.34191
p- ISSN 2528-1410 e- ISSN 2527-8045

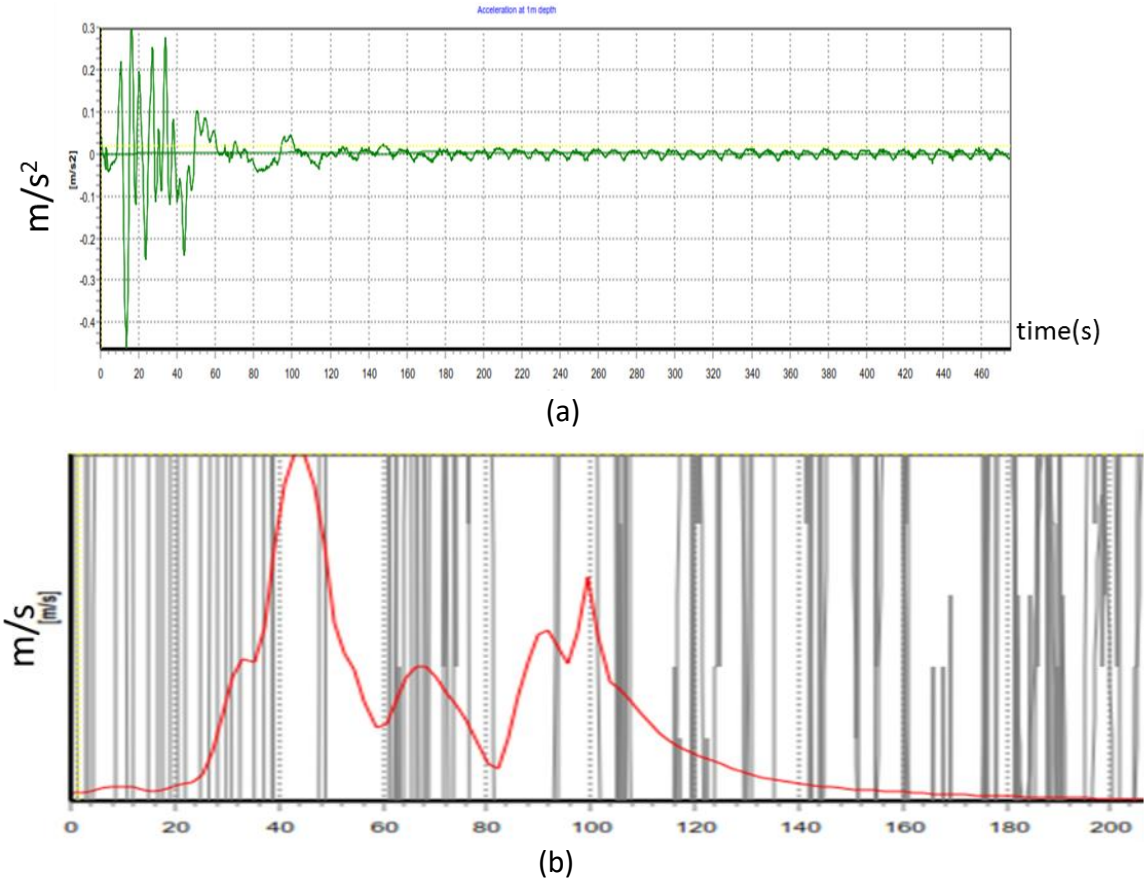

Figure 16. SCPT data for station FTB: (a) acceleration at 1 m depth and (b) frequency at 1 m depth (from FFT).

DOI: https://doi.org/10.17509/ijost.v6i2.34191
p- ISSN 2528-1410 e- ISSN 2527-8045

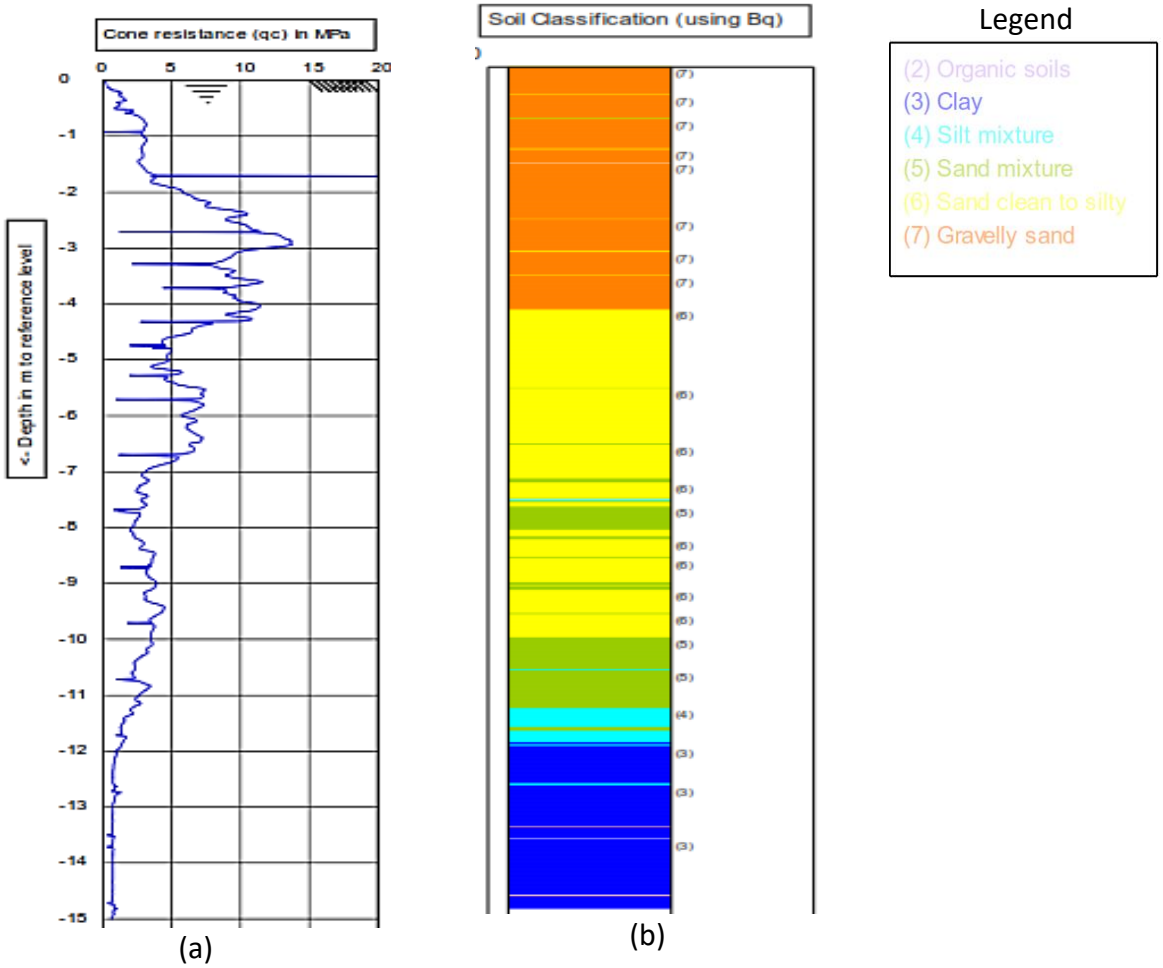

Figure 17. SCPT data for station UNP, (a) CPT sounding of SCPTu with cone resistance.

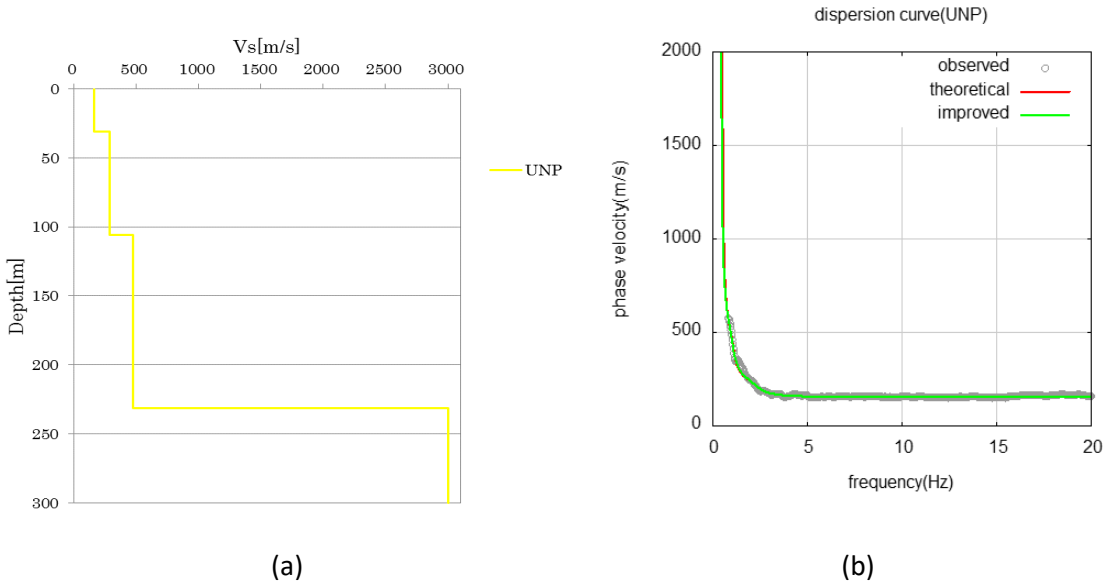

Figure 18. Microtremor array results: (a) Vs and depth; (b) dispersion curve for site UNP.

DOI:https://doi.org/10.17509/ijost.v6i2.34191
p- ISSN 2528-1410 e- ISSN 2527-8045

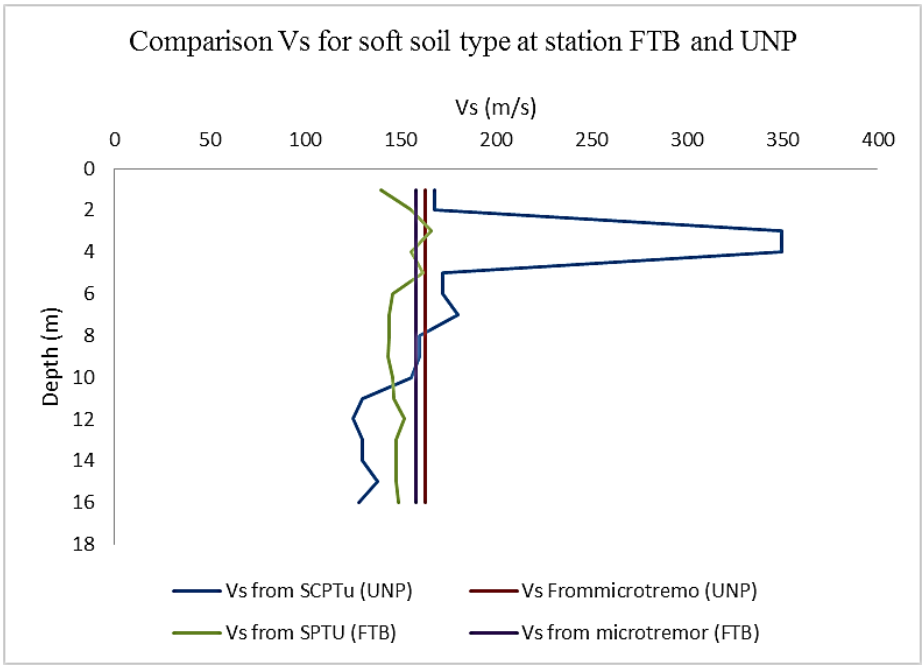

(a)

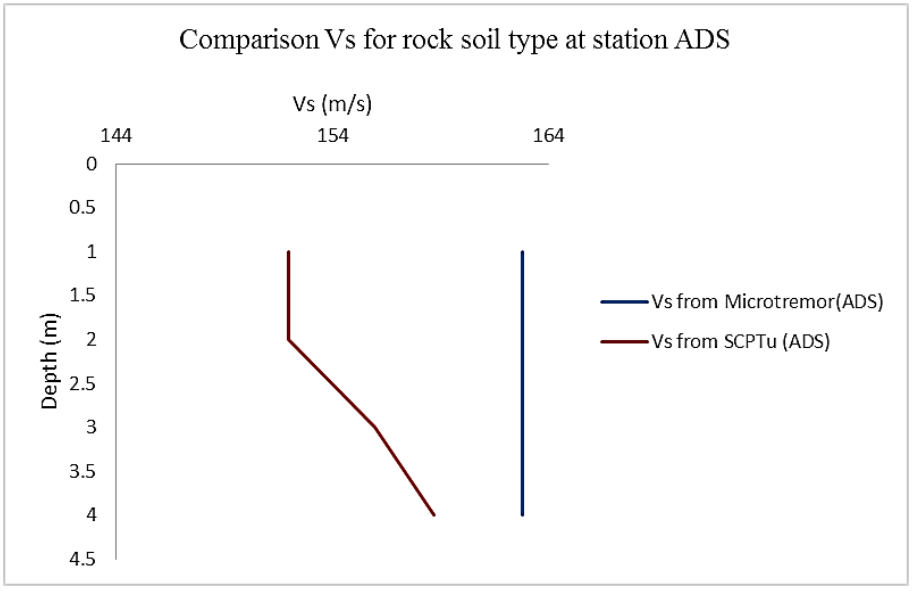

(b)

Figure 19. Comparison of Vs (a) for soft soil from station FTB and UNP, (b) for the rock soil type from station ADS.

DOI: https://doi.org/10.17509/ijost.v6i2.34191
p- ISSN 2528-1410 e- ISSN 2527-8045

Table 2. The comparison of Vs results.

Depth (m)	SCPTu			Microtremor array		
	ADS (m/s)	FTB (m/s)	UNP(m/s)	ADS (m/s)	FTB (m/s)	UNP(m/s)
0-2	145	152	163	308	165	163.5
2 -4	145	160	350	308	165	163.5
4 – 6	-	145	175	308	165	163.5
6 – 8	-	143	170	308	165	163.5
8 – 12	-	148	130	308	165	163.5

4. RESULTS AND DISCUSSION

4.1 Results

Figure 14 (a) and **(b)** presents acceleration data at 1 m depth and the FFT of acceleration, the predominant period of acceleration was 0.26s. By following the same procedure, each predominant period was determined at every 1 m increment for station ADS (rock type). **Figure 16 (a)** and **(b)** presents acceleration data at 1 m depth and the FFT of acceleration. From FFT the predominant period of acceleration was found to be 0.26s. The predominant period was determined for every 1 m increment at station FTB by following the same procedure for station UNP at station UNP, as shown in **Figure 17**, the Vs ranges from 0 to 15m. The Vs changed rapidly from 2m to 3.5m (sand to gravel, whereas the Vs of gravel was >300m/s) and the cone resistant value ranged from 7 MPa to 13 MPa. **Figure 19 (a)** indicates that the microtremor array result is unable to determine dramatic changes of Vs at the same layer as station UNP at 2 to 3.5m deep. The various soil properties at every depth (m) can be seen in Figure 17 (b).

The Vs profiles result obtained difference methods; from microtremor array and SCPTu on 3 site with difference soil types, The Vs profiles are not comparable due to their difference in resolution. While the SCPTu is able at every 1m depth up to cone's maximum penetration resistance, the microtremor array is more suitable for deeper measurement but with lower resolution. By considering constrain the inversion process, it can improve the resolution for Vs from microtremor array method. Our conclusions are based on comparing Vs between the microtremor array and SCPTu results with a limited number of observation sites (three in total: two for soft soil types and one for the rock type).

4.2. Discussion

The various techniques used to determine Vs (Tavakoli *et al.*, 2016), (Fatehnia *et al.*, 2015) in the field generally performed well. The comparison obtained Vs from microtremor and Borehole shows phase velocities with the dispersion curve calculated from the velocity structure was found that observations agree with borehole results to better than 11% except when the wavelength is greater than 2 times the array aperture (Hsi-Ping Liu, 2020).

These result show the conducted survey by SCPTu for three sites are The Vs profiles are not comparable due to their difference in resolution. While the SCPTu is able at every 1m depth up to cone's

DOI: https://doi.org/10.17509/ijost.v6i2.34191
p- ISSN 2528-1410 e- ISSN 2527-8045

maximum penetration resistance, the microtremor array is more suitable for deeper measurement but with lower resolution. The depth of penetration of SCPT was up to 18 m because the cone could not penetrate further upon reaching the maximum capacity of 22 MPa (McGann *et al.*, 2015). In some cases, this maximum was not achieved owing to a combination of high friction due to stiff clay, high tip resistance, or high friction in the Pleistocene sands.

The other result shows the microtremor array result is not suitable for shallow measurement compare with SPTu. The clearest case was station UNP, where the top 2 to 3.5m was hard material (Vs >300m/s), while the opposite result was found for shear velocity from the microtremor array technique, leading to generalized Vs= 163.6m/s from 0-30.9 depth (no change at 30m depth, called layer 1). In this location, the dispersion could be determined down to approximately 1 Hz, but the modelling indicated that it only obtained information from the top 15 m (**Figure 16**).

Microtremor array is more suitable for deeper measurement with lower resolution (Sant *et al.*, 2018). By considering constrain the inversion process, it can improve the resolution for Vs from microtremor array method (Yoshida & Uebayashi, 2021).

5. CONCLUSION

The shear velocity results from the microtremor studies were used to classify Padang soils into soft soils, medium soils and rock. The seismic cone penetration test unit (SCPTu) was used up to a depth of 18 m for the soft soil type and 4 m for the rock type. Comparison of the V_s for different soils type at the first layer between the microtremor array observation results and the SCPTu results indicated The compared the Vs profile within the first ~20m, as obtained from the microtremor array and the SCPTu. However, the accuracy of the Vs profile from the microtremor array is highly ambiguous. It is a known fact that microtremor techniques are not reliable in the near-surface due to the lack of high frequency data. Consequently, it is not surprising that the Vs profiles have poor resolution, in particularly at shallow depths, the microtremor array is more suitable for deeper measurement but with lower resolution. The resolution could have been improved by constraining the inversion process. On the hand, the SCPTu Vs profile returns a far better resolution because it is considered as an intrusive active seismic test and the signals were acquired at a depth interval of 1m.

6. ACKNOWLEDGEMENT

The authors would like to send high appreciate and thanks to DIKTI for financial support during conducting research in Padang and Ottawa University, Canada, Contract number 1248/E4.2/PP/2015. Thanks addressed to Dr. Totoh Andayono, Mr. Adit, Mr. Ari and Mr. Jamil for their contribution during conducting field survey. finally, High appreciate and thanks to Universitas Negeri Padang for final support through International research collaboration and penelitian dasar schemes PNBP with contract number 1012/UN35.13/LT/2021 and 904/UN35.13/LT/2021.

7. AUTHORS' NOTE

Authors declare that there is no conflict of interest regarding the publication of this article. Authors

DOI: https://doi.org/10.17509/ijost.v6i2.34191
p- ISSN 2528-1410 e- ISSN 2527-8045

confirmed that the paper was free of plagiarism.

8. REFERENCES

Carniel, R., Barazza, F., and Pascolo, P. (2006). Improvement of Nakamura technique by singular spectrum analysis. *Soil Dynamics and Earthquake Engineering*, *26*(1), 55-63.

Kennedy, J., and Eberhart, R. (1995). Particle swarm optimization. *Proceedings of ICNN'95-international conference on neural networks*, *4*(1995), 1942-1948.

Fatehnia, M., Hayden, M., and Landschoot, M. (2015). Correlation between shear wave velocity and SPT-N values for North Florida soils. *Electronic Journal of Geotechnical Engineering*, *20*(22), 12421-12430.

Lanin, D., Hermon, D., Fatimah, S., and Putra, A. (2019, August). A dynamics condition of coastal environment in Padang City-Indonesia. In *IOP Conference Series: Earth and Environmental Science*, *314*(1), 012006. IOP Publishing.

Genrich, J. F., Bock, Y., McCaffrey, R., Prawirodirdjo, L., Stevens, C. W., Puntodewo, S. S. O., and Wdowinski, S. (2000). Distribution of slip at the northern Sumatran fault system. *Journal of Geophysical Research: Solid Earth*, *105*(B12), 28327-28341.

Juliafad, E., Gokon., Putra, Rusnardi Rahmat., (2021). Defect study on single storey reinforced concrete building in West Sumatra: Before and after 2009 west. *International Journal of GEOMATE*, *20*(77), 205–212.

Khazaei, J., Amiri, A., and Khalilpour, M. (2017). Seismic evaluation of soil-foundation-structure interaction: Direct and Cone model. *Earthquakes and Structures*, *12*(2), 251-262.

McGann, C. R., Bradley, B. A., Taylor, M. L., Wotherspoon, L. M., and Cubrinovski, M. (2015). Development of an empirical correlation for predicting shear wave velocity of Christchurch soils from cone penetration test data. *Soil Dynamics and Earthquake Engineering*, *75*, 66-75.

Nakamura, Y. (2000, January). Clear identification of fundamental idea of Nakamura's technique and its applications. In *Proceedings of the 12th world conference on earthquake engineering*, *24*, 25-30. New Zealand: Auckland.

Natawidjaja, D. H., and Triyoso, W. (2007). The Sumatran fault zone—From source to hazard. *Journal of Earthquake and Tsunami*, *1*(01), 21-47.

Noguchi, T., Ono, Y., Kiyono, J., Horio, T., Kubo, M., Ikeda, T., and Putra, R. R. (2010). Determination of the subsurface structure of Padang City, Indonesia using microtremor exploration. *Journal of Japan Society of Civil Engineers, Ser. A1 (Structural Engineering and Earthquake Engineering (SE/EE))*, *66*(1), 30-39.

Noorlandt, R., Kruiver, P. P., de Kleine, M. P., Karaoulis, M., de Lange, G., Di Matteo, A., and Doornhof, D. (2018). Characterisation of ground motion recording stations in the Groningen gas field. *Journal of seismology*, *22*(3), 605-623.

DOI: https://doi.org/10.17509/ijost.v6i2.34191
p- ISSN 2528-1410 e- ISSN 2527-8045

Ono, Y., Noguchi, T., Rahmat Putra, R., Uemura, S., Ikeda, T., and Kiyono, J. (2012). Estimating subsurface shear wave velocity structure and site amplificatin characteristics of Padang, Indonesia. *Journal of Japan Society of Civil Engineers, Ser. A1 (Structural Engineering and Earthquake Engineering (SE/EE))*, *68*(4), I_227-I_235.

Parker, G. A., Baltay, A. S., Rekoske, J., and Thompson, E. M. (2020). Repeatable source, path, and site effects from the 2019 M 7.1 Ridgecrest earthquake sequence. *Bulletin of the Seismological Society of America*, *110*(4), 1530-1548.

Pradono, M. H. (2014). Kajian kerentanan gempabumi gedung bertingkat dengan bentuk beaturan dan tidak beraturan. *Jurnal Sains dan Teknologi Indonesia*, *16*(3), 20-25.

Prawirodirdjo, L., Bock, Y., Genrich, J. F., Puntodewo, S. S. O., Rais, J., Subarya, C., and Sutisna, D. S. (2000). One century of tectonic deformation along the Sumatran fault from triangulation and Global Positioning System surveys. *Journal of Geophysical Research: Solid Earth*, *105*(B12), 28343-28361.

Putra, R. R. (2017). Estimation of Vs30 based on soil investigation by using microtremor observation in Padang, Indonesia. *International Journal of Geomate*, *13*(38), 135-140.

Putra, R. R. (2020). Damage investigation and re-analysis of damaged building affected by the ground motion of the 2009 padang earthquake. *International Journal*, *18*(66), 163-170.

Putra, R. R. (2020). Relationship between obtained ultimate bearing capacity results based on n-spt results and static load tests. *International Journal*, *19*(74), 153-160.

Putra, R. R., Kiyono, J., Ono, Y., and Parajuli, H. R. (2012). Seismic hazard analysis for Indonesia. *Journal of Natural Disaster Science*, *33*(2), 59-70.

Putra, R. R., Kiyono, J., and Furukawa, A. (2014). Vulnerability assessment of non engineered houses based on damage data of the 2009 Padang earthquake in Padang city Indonesia. *International Journal of GEOMATE*, *7*(2), 1076-1083.

Rosyidi, A. P., Jamaluddin, T. A., Sian, L. C., and Taha, M. R. (2011). Earthquake impacts of the Mw 7.6, Padang, Indonesia, 30 September 2009. *Sains Malaysiana*, *40*(12), 1393-1405.

Sant, D. A., Parvez, I. A., Rangarajan, G., Patel, S. J., Salam, T. S., and Bhatt, M. N. (2018). Subsurface imaging of brown coal bearing Tertiary sedimentaries-Deccan Trap interface using microtremor method. *Journal of Applied Geophysics*, *159*, 362-373.

Sieh, K., and Natawidjaja, D. (2000). Neotectonics of the Sumatran fault, Indonesia. *Journal of Geophysical Research: Solid Earth*, *105*(B12), 28295-28326.

Sofyan, Y. (2016). Project for offshore Horizontal Directional Drilling (HDD) for pipeline crossing in Bukit Tua, Indonesia. *Indonesian Journal of Science and Technology*, *1*(2), 185-202.

Sutrisno, Putra, R. R., and Ganefri. (2017). A comparative study on structure in building using different partition receiving expense earthquake. *International Journal of Geomate*, *13*(37), 34-39.

DOI: https://doi.org/10.17509/ijost.v6i2.34191
p- ISSN 2528-1410 e- ISSN 2527-8045

Tavakoli, H. R., Amiri, M. T., Abdollahzade, G., and Janalizade, A. (2016). Site effect microzonation of Babol, Iran. *Geomechanics and Engineering*, *11*(6), 821-845.

Thein, P. S., Pramumijoyo, S., Brotopuspito, K. S., Wilopo, W., Kiyono, J., Setianto, A., and Putra, R. R. (2015, April). Designed microtremor array based actual measurement and analysis of strong ground motion at Palu city, Indonesia. In *AIP Conference Proceedings*, 1658(1), 040007

Thornley, J., Dutta, U., Fahringer, P., and Yang, Z. (2019). In situ shear-wave velocity measurements at the Delaney Park downhole array, Anchorage, Alaska. *Seismological Research Letters*, *90*(1), 395-400.

Wang, S. Y., Shi, Y., Jiang, W. P., Yao, E. L., and Miao, Y. (2018). Estimating Site Fundamental Period from Shear-Wave Velocity ProfileEstimating Site Fundamental Period from Shear-Wave Velocity Profile. *Bulletin of the Seismological Society of America*, *108*(6), 3431-3445.

Yoshida, K., and Uebayashi, H. (2021). Love-Wave Phase-Velocity Estimation from Array-Based Rotational Motion Microtremor. *Bulletin of the Seismological Society of America*, *111*(1), 121-128.

DOI: https://doi.org/10.17509/ijost.v6i2.34191
p- ISSN 2528-1410 e- ISSN 2527-8045